Eur. Phys. J. Special Topics **171**, 9–14 (2009)

DOI: 10.1140/epjst/e2009-01005-y

THE EUROPEAN PHYSICAL JOURNAL SPECIAL TOPICS

Regular Article

Vortex-antivortex pair in a Bose-Einstein condensate

Type-II quantum lattice gas as a nonlinear ϕ^4 theory of a complex field

J. Yepez[1], G. Vahala[2], and L. Vahala[3]

[1] Air Force Research Laboratory, Hanscom AFB, Massachesetts 01731, USA
[2] Department of Physics, William & Mary, Williamsburg, Virginia 23185, USA
[3] Department of Electrical & Computer Engineering, Old Dominion University, Norfolk, Virginia 23529, USA

Abstract. Presented is a type-II quantum algorithm for superfluid dynamics, used to numerically predict solutions of the GP equation for a complex scalar field (spinless bosons) in ϕ^4 theory. The GP equation is a long wavelength effective field theory of a microscopic quantum lattice gas with nonlinear state reduction. The quantum lattice gas algorithm for modeling the dynamics of the one-body BEC state in 3+1 dimensions is presented. To demonstrate the method's strength as a computational physics tool, a difficult situation of filamentary singularities is simulated, the dynamics of solitary vortex-antivortex pairs, which are a basic building block of morphologies of quantum turbulence.

1 Introduction

The physical behavior of a complex scalar field ϕ with an interaction Lagrangian density $\mathcal{L}_{\text{int}} \propto \phi^4$ is an extremely rich scalar field theory, applicable to a phase coherent Bose-Einstein condensate (BEC) at zero temperature. Here we study this ϕ^4 theory with low energy dynamics well described by the Gross-Pitaevskii (GP) equation in the mean-field limit [1,2], which is an effective nonlinear interaction model of a BEC and also an effective low energy equation of motion of a type-II quantum lattice gas system. In particular, we numerically demonstrate the solitary structure of quantized vortex line solutions of the GP equation. A prevailing application area of quantum turbulence is (1) in cold atomic gas BEC quantum systems and (2) as a precursory theory for understanding vortex tube morphological dynamics fundamental to fluid turbulence.

A variety of physically relevant quantum lattice gas systems have been recently developed by us, and these type-II quantum systems have emergent nonlinear effective equations of motion governing dynamical behavior of the low energy and low momentum modes. Satisfying the dual purposes of computational physics and quantum computation, these numerical quantum lattice models are strictly unitary and have proven useful for numerically predicting the time-dependent solutions of a wide class of effective nonlinear quantum wave equations. The method has previously been applied to the Korteveg de-Vries equation, a reduced set of magnetohydrodynamic equations, and various forms of the nonlinear Schroedinger (NLS) equation, including the Manakov equations for optical solitons and the GP equation for BECs in $2+1$ and $1+1$ dimensions [3]. Here, we treat the subject of solitary vortices (dark solitons) governed by the GP equation in $3+1$ dimensions, which are one of the basic morphological structures comprising quantum turbulence.

1.1 GP equation for superfluids

The NLS equation, also called the GP equation [1,2], is a mathematical model of superfluids, describing vortex nucleation and reconnections. It accurately describes the superfluid BEC phase, a compressible nonlinear quantum fluidic phase for weak 2-body interactions. For example, it is a good model of dilute atomic vapor BEC with vortex-sound interactions. Recently, over the last decade, BECs have been produced using rarefied cold atom vapors (dilute alkali gas) in magneto-optical particle traps and optical lattices (typical vapors have 10^6 to 10^7 atoms of ^{87}Rb, ^{7}Li, and ^{23}Na atoms). These have a stable condensate wave function larger than the noninteracting ground state of the trap.

Excitations of superfluid, such as ^{4}He, include (1) maxons and rotons in the high (atomic-scale) wave number range (short wavelength limit) and (2) phonons in the low wave number range (long wavelength limit). The GP equation contains only phonon excitations. In a finite temperature superfluid, such as the He II phase of ^{4}He, there are two fluids. At finite temperature there is also a normal fluid. Entangled vortex lines in the superfluid can interact with the normal fluid; Landau's mutual frictional process is one source of dissipation. In the GP equation, there is only one fluid, the superfluid component. So, mutual friction is not modeled.

The Madelung change of variables of the complex wave function $\phi = \sqrt{\rho}\, e^{i\theta}$, where the condensate number density $\rho = |\phi|^2$ is the fluid density and gradient of its phase $\mathbf{v} = 2\nabla\theta$ is the velocity, maps the GP equation $i\partial_t \phi = -\nabla^2\phi + |\phi|^2\phi$ to the fluid equation $\partial_t \boldsymbol{v} + \boldsymbol{v}\cdot\nabla\boldsymbol{v} = -\nabla P - \nabla V$, where $P = 2\rho$ is the pressure and $V = -2\frac{\nabla^2\sqrt{\rho}}{\sqrt{\rho}}$ is the Bohm quantum interparticle potential. The continuity equation $\partial_t\rho + \nabla\cdot(\rho\boldsymbol{v}) = 0$ comes from the imaginary part of the GP equation and the Bernoulli equation $-\partial_t\theta = (\nabla\theta)^2 + \frac{V}{2} + \rho$ comes from the real part.

The vorticity, the curl of the superfluid velocity $(2\nabla \times \nabla\theta)$, vanishes in a single-connected region of the fluid. A contour enclosing a vortex line has quantized circulation in units of 2π. The vortex core size is given by the healing length $1/\sqrt{g\rho}$, where g is the nonlinear coupling strength. Feynman proposed that the superfluid turbulent state consists of a tangle of quantized vortices [4]. Quantized vortices can decay by sound emission through vortex reconnections. Vortex lines are destroyed in two ways. (1) Emission of sound waves (compressible excitations) escape to infinity; this occurs in connection with the breaking and reconnection of vortex lines. (2) Transverse vortex waves (helical perturbations of the vortex tube away from it cylindrical shape) known as Kelvin waves are supported on the filamentary core with an energy cascade (large waves coupling to smaller waves) [5]; vortices reduce in a Richardson cascade [6] (large vortices break into smaller vortices) leading to the famous Kolmogorov spectrum $E(k) \propto \epsilon^{2/3}k^{-5/3}$. When the Richardson cascade is operative, vortex lines reduce down to elementary excitations at the healing length scale (analogous to the viscous dissipation scale). The topological operations are reconnection of vortices and disappearance of small vortex loops. Previous models used to study the GP equation include the vortex-filament model [7,8] and spectral decompositon models. The quantum lattice gas offers an alternative numerical solution method for type-II quantum computers.

2 Quantum lattice gas method

In a quantum lattice gas, the wave function of a many-body quantum system is resolved on a grid (a Bravais lattice), a typical type-II quantum algorithm with phase-coherent unitary operation of a small finite-quantum system at each lattice node and permutations of data between nodes (a classical communication network) [9]. No divergences typical in quantum field theories exist in our model because the finite grid size of the lattice provides a momentum cut-off to the quantum theory, removing high k-modes, and the lattice provides a spatial cut-off as the simulation is carried out in a finite-size box with periodic boundary conditions. Furthermore, the unitary quantum evolution, represented by quantum logic gates, ensures stable dynamics. The evolution operator governing the time-dependent behavior of the wave function is cast as a local algorithm with three steps applied in a time-interleaved fashion: (1) a classical stream operator for the site-to-site hopping, (2) a quantum collision operator for the on-site interactions, and (3) a state reduction operator for the ϕ^4 self-interaction, reducing computational expense.

With the first two homogeneous (spatially independent) stream and collide operators, we recover linear quantum theories, both non-relativistic and relativistic theories. The third inhomogeneous (spatially dependent) state reduction operator allows us to go further to model nonlinear systems, a primary advantage of type-II quantum computing. State reduction is represented by a gauge operation, related to the intrinsic nonlinear interaction potential.

To represent the GP equation, the quantum algorithm presented here uses a 2-spinor field on a cubic lattice. State reduction is represented as a gauge operations that depends on the wave function itself, rotating the phase of the spinor components. The usual quantum lattice gas method of splitting the dynamics between mutually exclusive stream and collide steps is employed, in a novel way appropriate for recovering continuous dynamics in three spatial dimensions, with second order accuracy in the scaling limit.

2.1 Quantum algorithm for the Schroedinger equation in $3+1$ dimensions

We consider a 2-spinor field $\psi(\boldsymbol{x},t) = \begin{pmatrix}\alpha(\boldsymbol{x},t)\\ \beta(\boldsymbol{x},t)\end{pmatrix}$, where α and β are complex amplitudes. The quantum operator $C = \frac{1}{2}\begin{pmatrix}1-i & 1+i\\ 1+i & 1-i\end{pmatrix}$ acts locally at every $\boldsymbol{x}$, entangling each pair of the spinor amplitudes, by the map

$$\psi = C\psi. \tag{1}$$

Because $\begin{pmatrix}1\\1\end{pmatrix} = C\begin{pmatrix}1\\1\end{pmatrix}$, the complex scalar density $\phi = (1,1)\cdot\psi = \alpha+\beta$ is conserved by (1), and consequently the probability $|\psi|^2$ is also conserved locally. Local equilibrium occurs when the amplitudes are equal ($\alpha = \beta$), but in general such a local equilibrium is then broken if a spinor component is displaced in space by the vectorial amount $\Delta\boldsymbol{x}$. To conserve probability, we admit only complementary displacements of the spinor components, induced by the standard stream operators of the form $S_{\Delta\boldsymbol{x},0} = n + e^{\Delta\boldsymbol{x}\partial_{\boldsymbol{x}}}\bar{n}$ and $S_{\Delta\boldsymbol{x},1} = \bar{n} + e^{\Delta\boldsymbol{x}\partial_{\boldsymbol{x}}}n$, where $n = \begin{pmatrix}0 & 0\\ 0 & 1\end{pmatrix}$ and $\bar{n} = \mathbf{1} - n$. That is, the stream operators act on the 2-spinor as follows:

$$S_{\Delta\boldsymbol{x},0}\psi(\boldsymbol{x}) = \begin{pmatrix}\alpha(\boldsymbol{x}+\Delta\boldsymbol{x})\\ \beta(\boldsymbol{x})\end{pmatrix} \quad S_{\Delta\boldsymbol{x},1}\psi(\boldsymbol{x}) = \begin{pmatrix}\alpha(\boldsymbol{x})\\ \beta(\boldsymbol{x}+\Delta\boldsymbol{x})\end{pmatrix}. \tag{2}$$

Although the application of (2) usually breaks local equilibrium induced by (1), with the appropriate boundary conditions, for example periodic boundary conditions, (2) is guaranteed to conserve the total density $\int d^3x\,\psi(\boldsymbol{x})$, and in turn the total probability $\int d^3x(|\alpha(\boldsymbol{x})|^2+|\beta(\boldsymbol{x})|^2)$. To construct a quantum algorithm, any combination of the operators C and $S_{\Delta\boldsymbol{x},\sigma}$, for $\sigma = 0$ or 1, and the respective adjoints, are suitable from the point of conservation. However, we restrict our considerations to those combinations which are close to the identity operator. Our basic approach uses the interleaved operator

$$I_{x\sigma} = S_{-\Delta\boldsymbol{x},\sigma}C^\dagger S_{\Delta\boldsymbol{x},\sigma}C \tag{3}$$

as the basic building block of our quantum algorithm. For example, an evolution operator for the spinor component σ is

$$U_\sigma[\Omega(\boldsymbol{x})] = I_{x\sigma}^2 I_{y\sigma}^2 I_{z\sigma}^2 e^{-i\varepsilon^2\Omega(\boldsymbol{x})}, \tag{4}$$

where $\varepsilon \sim \frac{1}{N}$, where N is the grid resolution (*i.e.* N is the number of grid points along one edge of the simulation volume). (4) represents the three aspects of a type-II quantum algorithm: stream, collide, and state reduction. In dimensionless units ($c = 1$), note that $\varepsilon^2 \sim \Delta x^2 \sim \Delta t$. This evolution operator is spatially dependent only through local state reduction Ω:

$$\psi(\boldsymbol{x}, t+\Delta t) = U_\sigma(\boldsymbol{x},\Omega)\psi(\boldsymbol{x},t). \tag{5}$$

The R.H.S. of (5) is a finite-difference of ψ, which is too long to write out here. If we Taylor expand the R.H.S. in ε, we obtain the following quantum lattice gas equation

$$\begin{pmatrix}\alpha'\\ \beta'\end{pmatrix} = \begin{pmatrix}\alpha\\ \beta\end{pmatrix} + i\frac{\varepsilon^2}{2}\nabla^2\begin{pmatrix}\beta\\ \alpha\end{pmatrix} - i\varepsilon^2\Omega\begin{pmatrix}\alpha\\ \beta\end{pmatrix} + \frac{(-1)^\sigma\varepsilon^3}{4}\nabla^3\begin{pmatrix}\alpha - i\beta\\ -\beta + i\alpha\end{pmatrix} + \mathcal{O}(\varepsilon^4), \tag{6}$$

with $\begin{pmatrix}\alpha'\\ \beta'\end{pmatrix} = \psi(\boldsymbol{x}, t + \Delta t)$ and where $\sigma = 0$ or 1. Using the Pauli matrices $\sigma_x = \begin{pmatrix}0 & 1\\ 1 & 0\end{pmatrix}$, $\sigma_y = \begin{pmatrix}0 & -i\\ i & 0\end{pmatrix}$, and $\sigma_z = \begin{pmatrix}1 & 0\\ 0 & -1\end{pmatrix}$, then (6) can be written

$$\psi(\boldsymbol{x}, t + \Delta t) = \psi(\boldsymbol{x}, t) - i\varepsilon^2\left[-\frac{1}{2}\sigma_x\nabla^2 + \Omega\right]\psi(\boldsymbol{x}, t) + \frac{(-1)^\sigma\varepsilon^3}{4}(\sigma_y + \sigma_z)\nabla^3\psi(\boldsymbol{x}, t) + \mathcal{O}(\varepsilon^4). \tag{7}$$

Since the order ε^3 error term in (6) changes sign with σ, we can induce a cancelation of this error term using a symmetric evolution operator

$$U[\Omega] = U_1\left(\frac{\Omega}{2}\right)U_0\left(\frac{\Omega}{2}\right) \tag{8a}$$

that is invariant under spin component interchange.[1] Therefore, the following quantum map $\psi(\boldsymbol{x}, t + \Delta t) = U[\Omega(\boldsymbol{x})]\psi(\boldsymbol{x}, t)$ leads to the quantum lattice gas equation

$$\psi(\boldsymbol{x}, t + \Delta t) = \psi(\boldsymbol{x}, t) - i\varepsilon^2\left[-\frac{1}{2}\sigma_x\nabla^2 + \Omega\right]\psi(\boldsymbol{x}, t) + \mathcal{O}(\varepsilon^4). \tag{9}$$

Now, in the low energy scaling limit, we have $\partial_t\psi(\boldsymbol{x}, t) = \frac{1}{\varepsilon^2}[\psi(\boldsymbol{x}, t + \Delta t) - \psi(\boldsymbol{x}, t)]$. Therefore, dividing both sides of (9) by ε^2, the quantum lattice gas equation is

$$i\partial_t\psi = -\sigma_x\nabla^2\psi + \Omega\psi + \mathcal{O}(\varepsilon^2) \tag{10}$$

in the low energy and low momentum limit. Finally, since $\phi = \alpha + \beta$, taking the density moment gives the effective scalar field equation

$$i\partial_t\phi = -\nabla^2\phi + \Omega\phi + \mathcal{O}(\varepsilon^2), \tag{11}$$

which is the Schroedinger wave equation with $m = \frac{1}{2}$ for $\hbar = 1$, so long as $|\Delta\boldsymbol{x}|^2 = \Delta t = \varepsilon$. From the order of the error term in (11), the Taylor expansion predicts that the quantum algorithm is second order convergent in space.

The low energy effective Hamiltonian that generates the evolution, $U = e^{i\Delta t H_{\text{eff}}/\hbar}$, is the following $H_{\text{eff}} = -\frac{\hbar^2}{2m}\nabla^2 + \hbar\Omega(\boldsymbol{x}) + \mathcal{O}(\Delta t, \Delta x^2)$, where we have written the quantum diffusion coefficient as $\frac{\Delta x^2}{\Delta t} = \frac{\hbar}{m}$. This is the nonlinear GP Hamiltonian since $\hbar\,\Omega(\boldsymbol{x}) = g|\phi(\boldsymbol{x})|^2$, where g the on-site interaction energy.

3 Solitary vortex-antivortex dynamics

Here we present some simulations of vortex reconnection and break-up for the GP Hamiltonian demonstrating the emission of Kelvin waves along the vortex tubes well before reconnection.

[1] As an alternative to (8a), we can use the interleaved operator $I_{x\sigma} = S_{-\Delta\boldsymbol{x},\sigma}CS_{\Delta\boldsymbol{x},\sigma}C$, in terms of which the evolution operator is cast as

$$U[\Omega] = I_{x0}^2 I_{y1}^2 I_{z0}^2 e^{-i\varepsilon^2\Omega(\boldsymbol{x})/2} I_{z1}^2 I_{y0}^2 I_{x1}^2 e^{-i\varepsilon^2\Omega(\boldsymbol{x})/2}. \tag{8b}$$

This is a direct extension to 3+1 dimensions of the quantum algorithm for the NLS equation presented in an earlier paper [3] for the 2+1 dimensional case. (8b) also models (11).

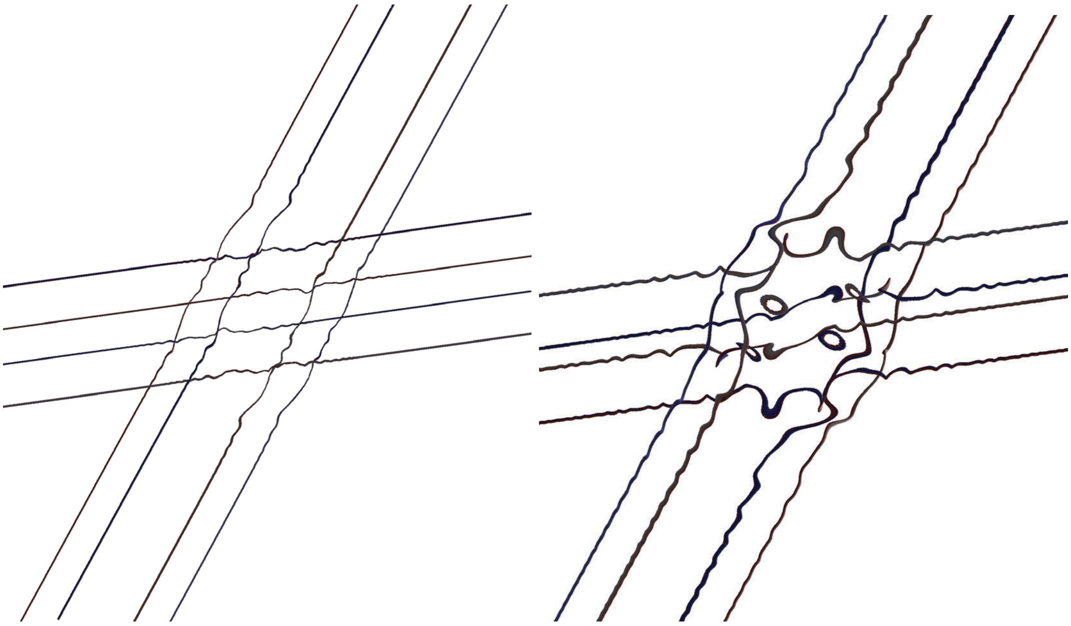

Fig. 1. Simulation of vortex and anti-vortex filaments, originally linear and oriented perpendicularly on a 1024^3 grid. Time steps $t = 1200\Delta t$ and $t = 4800\Delta t$ are plotted. Kelvin waves are seen along the vortex filaments early in the simulation. At the late stages, the filaments bend, reconnect, and exchange vortex rings.

This kind of reconnection [10] occurs here even in the absence of viscosity and resistivity because for quantized vortices the density vanishes, $|\phi|^2 \to 0$, at the vortex core. To ensure a perturbative phase, we consider the GP equation in the form

$$i\partial_t \phi = -\nabla^2 \phi + (|\phi|^2 - a_\infty)\phi \tag{12}$$

with $\phi \to \sqrt{a_\infty}$ as $r \to \infty$. The reason for choosing the bulk density of the scalar field to be $|\phi|^2 = a_\infty$ is two-fold. (1) With this choice, the GP interaction term vanishes in (12). Hence, in the bulk region away from the vortex center, the quantum fluid essentially behaves as a free quantum field. (2) a_∞ can then be factored out of the GP interaction term, so the spacetime parabolic (non-relativistic) scaling $x \to \sqrt{a_\infty} x$ and $t \to a_\infty t$ provides a pathway to normalization of the wave function, to unity say. This kind of wave function normalization is numerically preferable, since it allows one to resolve the vortex core with an arbitrary number of spacetime lattice points. Following Berloff [11], a Padé asymptotic representation can be found for a simple vortex parallel to the z-axis. Using cylindrical coordinates one seeks a radial Padé solution of in the form $\phi = R(r)e^{i\theta}$ with

$$R(r) = \sqrt{\frac{r^2(a_1 + a_\infty b_2 r^2)}{1 + b_1 r^2 + b_2 r^4}}, \tag{13}$$

with the solution $a_1 = 11a_\infty^2/32$, $b_1 = a_\infty/3$, $b_2 = a_1/12$. Figures 1 and 2 show examples of the reconnection processes, a view on a 1024^3 grid and a zoomed in view on a 240^3 grid, respectively. The smallest grid we have been successfully able to run the quantum lattice gas model is 80^3. If the grid is too small, numerical artifacts occur due to the error terms in the effective field theory, leading to unphysical oscillations of the vortex filaments.

4 Final remarks

Magnetically trapped alkali vapors, have an external parabolic trapping potential, usually of the asymmetric form $V(\boldsymbol{x}) = kr^2$, where $r = \sqrt{\gamma_x x^2 + \gamma_y y^2 + \gamma_z z^2}$, where the gamma coefficients

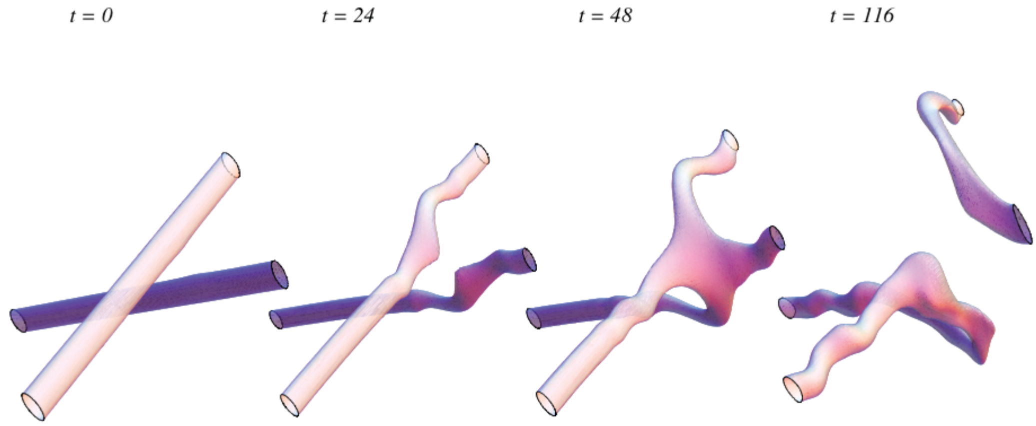

Fig. 2. Time development vortex-antivortex reconnection on a 240^3 grid. One octant at each time step is shown for clarity. At $t = 0$ (left), two independent vortex lines, oriented perpendicularly and separated in space (non-intersecting cores). By $t = 24$, the vortex-pair becomes unstable, inducing traveling Kelvin waves along the filamentary core. At $t = 48$, the two vortex cores connect. By $t = 116$ (right), the cores are disconnected along the original orientations, and are then reconnected into two separate filaments, each turned at right angles, with the induced Kelvin waves clearly apparent.

are not all equal. It is straightforward to add a confining potential in the model. However, the vortex-antivortex simulations are more difficult to carryout because, without a confining potential, perfect continuity of the wave function across the periodic boundaries must occur at all times for both the amplitude and the phase of the BEC wave function. With an external trapping potential, the condensate wave function need not be periodic. Hence, we chose to demonstrate the usefulness of the quantum algorithm in $3 + 1$ dimensions with a difficult test case capturing vortex dynamics.

The algorithmic complexity of our approach is strictly a function of the grid size needed to resolve the quantum flow. Irregular external potentials, for example those representing time-dependent field effects, including fringe fields, can be modeled with the type-II quantum lattice gas method without extra algorithmic complexity.

We thank the Air Force Office of Scientific Research. JY would like to thank lieutenants J. Scoville, M. Kripchak, and J. Torgerson for assistance in verifying the quantum lattice gas algorithm in $3 + 1$ dimensions, running simulation tests of harmonic oscillator energy eigenstates, with excellent comparison to a pseudo-spectral method. We would like to thank M. Soe for the parallel version of the code and S. Ziegeler for parallel graphics code. Finally, we thank the Naval Oceanographic Office and the Air Force Research Laboratory's High Performance Computing Major Shared Resource Centers for supercomputer allocations.

References

1. E.P. Gross, J. Math. Phys. **4**, 195 (1963)
2. L.P. Pitaevskii, Soviet Phys. JETP **13**, 451 (1961)
3. J. Yepez, G. Vahala, L. Vahala, Quant. Inform. Process. **4**, 457 (2005)
4. R.P. Feynman, *Progress in Low Temperature Physics*, Vol. I (North-Holland, Amsterdam, 1955)
5. D. Kivotides, J.C. Vassilicos, D.C. Samuels, C.F. Barenghi, Phys. Rev. Lett. **86**, 3080 (2001)
6. L.F. Richardson, Proc. Royal Soc. London, Series A, **110**, 709 (1926)
7. K.W. Schwarz, Phys. Rev. B **31**, 5782 (1985)
8. K.W. Schwarz, Phys. Rev. B **38**, 2398 (1988)
9. J. Yepez, Int. J. Mod. Phys. C **12**, 1273 (2001)
10. J. Koplik, H. Levine, Phys. Rev. Lett. **71**, 1375 (1993)
11. N.G. Berloff, J. Phys. A **37**, 1617 (2004)